The submitted manuscript has been authored by a contractor of the U.S. Government under contract No. W-31-109-ENG-38. Accordingly, the U.S. Government retains a nonexclusive, royalty-free license to publish or reproduce the published form of this contribution, or allow others to do so, for U.S. Government purposes.

CONF-9009329--/
ANL-HEP-CP
For the Proc
Workshop PP
Protvino, US
25-28 Septem

ANL-HEP-CP-90-103
For the Proceedings of the Workshop "Physics at UNK" Protvino, USSR 25-28 September 1990

The Fermilab Polarized Beam Facility*

D. P. Grosnick[†]
High Energy Physics Division
Argonne National Laboratory
Argonne, IL 60439

ANL-HEP-CP--90-103
DE91 006556

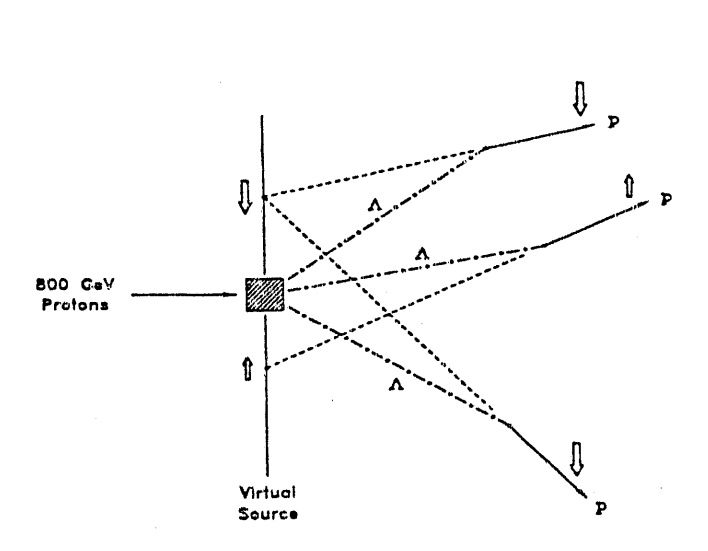
Abstract

A description¹ of the Fermilab 200-GeV/c polarized beam is presented, including the production, transport, and spin rotation of the polarized protons and antiprotons. The momentum and polarization of each beam particle is measured by a beam-tagging system. Verification of the beam polarization and of the beam-tagging method is given by two polarimeters. A brief summary of the E-704 experimental program using the polarized beam is also presented.

A. The Polarized Beam

The polarized proton beam is produced from the parity-nonconserving decay, $\Lambda^0 \to p + \pi^-$. As viewed in the Λ rest frame, the proton spin is aligned in the same direction as the proton's momentum. For unpolarized Λ particles, the polarization of the proton has been measured² to be 64%. This value comes from the interference of S and P-wave amplitudes.

As shown in Fig. 1, an 800-GeV incident proton beam from the Tevatron hits a beryllium target and produces many particles in the collision, including both Λ and $\overline{\Lambda}$ hyperons. The unpolarized Λ particles then decay some distance downstream from the target. In the laboratory frame, the proton trajectory from this decay can be traced back to the plane of the target. The protons then appear to originate from a virtual source at the target. A correlation exists between the transverse distance from the target and the proton trajectory, which in turn is correlated to the proton spin direction. The correlation between the horizontal transverse distance from the target and the proton polarization is shown in Fig. 2. Protons with the same transverse spin component appear to originate



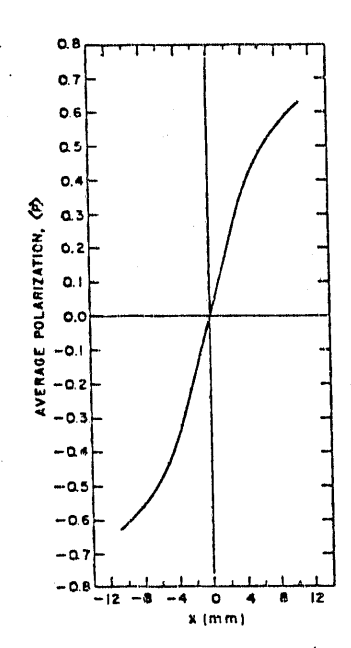


Figure 1: Diagram of the production target and Λ decays, showing the virtual source of polarized protons.

Figure 2: Correlation between the average particle polarization and the horizontal position.

from the same point on the virtual source. The larger proton polarization values are located further from the center of the target because the proton trajectories are closer to 90° from the Λ momentum direction. Polarized antiprotons are produced in a completely similar manner from $\overline{\Lambda}$ decays.

The primary goal of the polarized beam transport system is to create no net spin precession, which then preserves the correlation between the proton polarization state and the position located at the virtual source. This goal is accomplished by using four quadrupole doublet magnets, shown as the four lenses in Fig. 3. The beam line is mirror symmetric about an intermediate focus, and the four sets of quadrupole doublets are used to correct depolarization effects. The intermediate focus, where the beam-tagging occurs, is located 160 m downstream of the production target, and the final focus, where the experimental target is situated, is 320 m downstream of the production target. The beam particle trajectory at the final focus is designed to be the same as that at the virtual source. The actual intermediate focus location depends on the momentum of the beam particle. Higher-momentum particles focus further downstream of the central-momentum location, and lower-momentum particles focus farther upstream. Each set of four dipole magnets that bend the beam produces no net momentum dispersion and no net particle spin rotation. The polarized antiproton beam is transported in exactly the

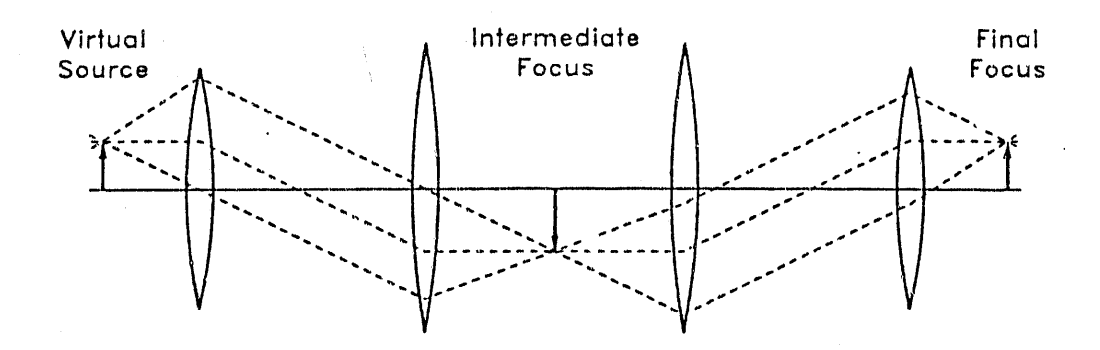


Figure 3: Diagram illustrating the polarized beam optics.

same way, with only the polarities of the beam-line magnets reversed.

A side view of the polarized beam line is given in Fig. 4. The noninteracting 800-GeV primary beam and other unwanted charged particles are swept away from the beam by two dipole magnets. The distance between 9 and 30 m downstream of the production target is the Λ decay region, where polarized protons are produced. Unwanted neutral particles such as neutrons are absorbed in a neutral dump, while the polarized proton beam is bent below the dump. Just upstream of the intermediate focus location, a collimator limits the momentum of the beam to $\pm 9\%$ of the nominal 200 GeV/c. At the intermediate focus region, each beam particle has its momentum and polarization measured by a beam-tagging system. An unwanted 13% pion contamination from inflight kaon decays is identified by two beam Čerenkov counters. Before interacting with the experimental target, the direction of the protons may be rotated by a series of magnets referred to as a "Siberian snake."

The snake magnet system has four requirements: (1) rotate the spin direction from the horizontal (S) to the longitudinal (L) or to the vertical (N) directions, (2) reverse the spin direction of the beam particles, which minimizes systematic errors, by reversing the magnet polarity, (3) create no net beam steering, which introduces no net change in the beam particle trajectory, and (4) produce no optical distortion, which minimizes depolarizing effects. The spin-rotation system consists of 12 dipole magnets whose fields are transverse to the beam direction and tilted at 45° to the vertical axis. Each magnet precesses the particle spin by 45°. Two different combinations of the 12 magnets allow for the rotation from the $S \to L$ spin direction and from the $S \to N$ spin direction. Tests of the spin-rotation magnets indicate that the system works as designed.

The polarized beam parameters are listed in Table I. The given values assume an incident primary beam intensity of 1×10^{12} protons per 20-sec spill at an energy of

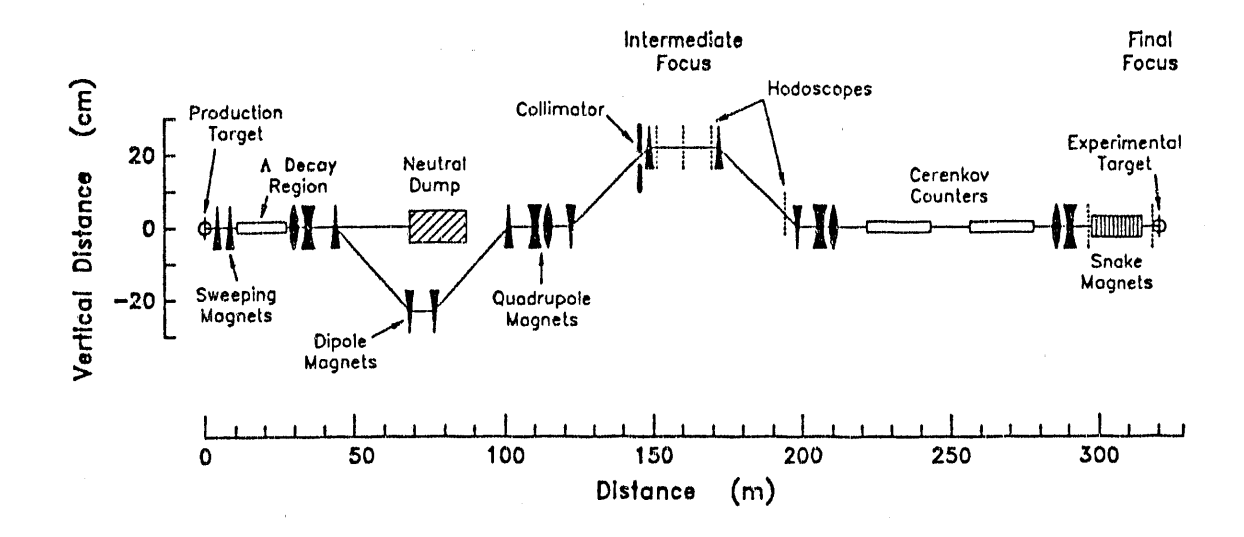


Figure 4: Side view of the Fermilab polarized beam line.

Parameter	Protons	Antiprotons
Beam momentum, (Gev/c)	200	200
Intensity, (polarized particles per 20-sec spill)	9×10^6	5×10^5
Tagged particles with magnitude > 0.35, (polarized particles per 20-sec spill)	3×10^6	1.6×10^5
Average tagged polarization	45%	45%
Beam content	$p/\pi^{+} = 9/1$	$\overline{p} / \pi^- = 1 / 5$

Table 1: List of polarized proton and antiproton beam parameters using a primary proton beam with an energy of 800 GeV and an average intensity of 1×10^{12} protons per 20-sec spill.

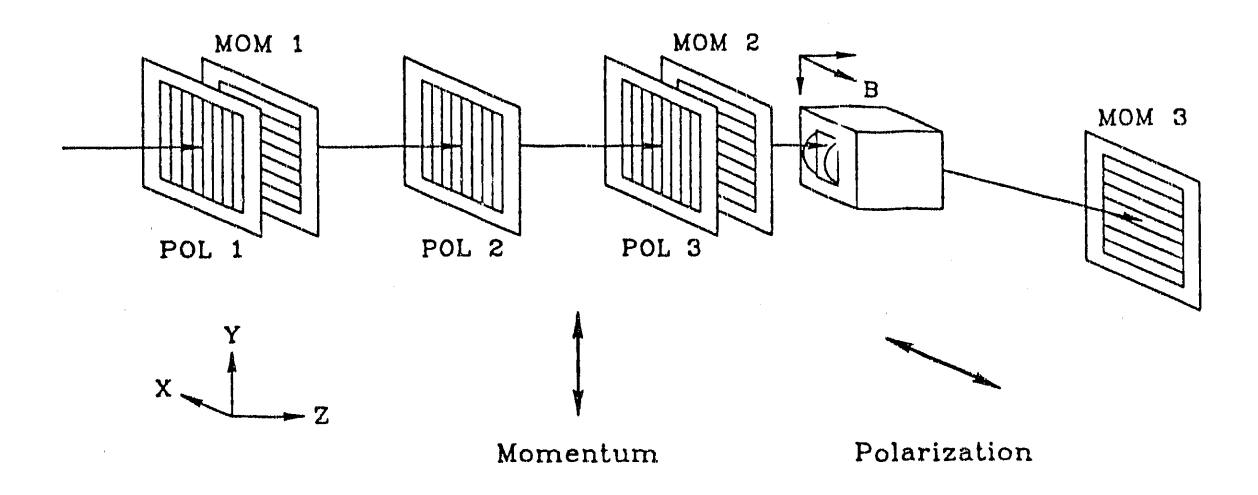


Figure 5: Diagram showing the beam-tagging scintillator hodoscopes.

800 GeV. The difference in production rate between protons and antiprotons is 1/18. The beam profile at the final focus is 2 cm (FWHM) in the horizontal width and 3 cm (FWHM) in the vertical. Both signs of the beam particle polarization are present at the same time.

A similar design for polarized proton and antiproton beams have been proposed for the POLEX experiment at UNK.

B. The Beam-Tagging System

Since the polarized protons originate from Λ decays, there are many possible values of the momentum and polarization. Each beam particle is tagged to determine its polarization value, using the correlation between the position and the polarization state. The momentum of the beam particle is measured in the vertical direction, from which the intermediate focus location along the beam line is calculated. By measuring the horizontal position of the beam-particle trajectory at this intermediate focus, the value of the polarization for that particle is determined by the correlation.

The beam-tagging system at the intermediate focus consists of 6 scintillation counter hodoscopes to determine a position in both the horizontal and the vertical directions, as shown in Fig. 5. The hodoscopes, labeled MOM1 and MOM2, determine the trajectory before entering an analyzing magnet. The vertical position afterwards is measured by MOM3. By comparing the measured angle of deflection with an angle given by a known trajectory, the momentum can be determined. The hodoscopes POL1 and POL3 measure the beam trajectory in the horizontal direction, and from this the polarization can then be found. The momentum and polarization information is given

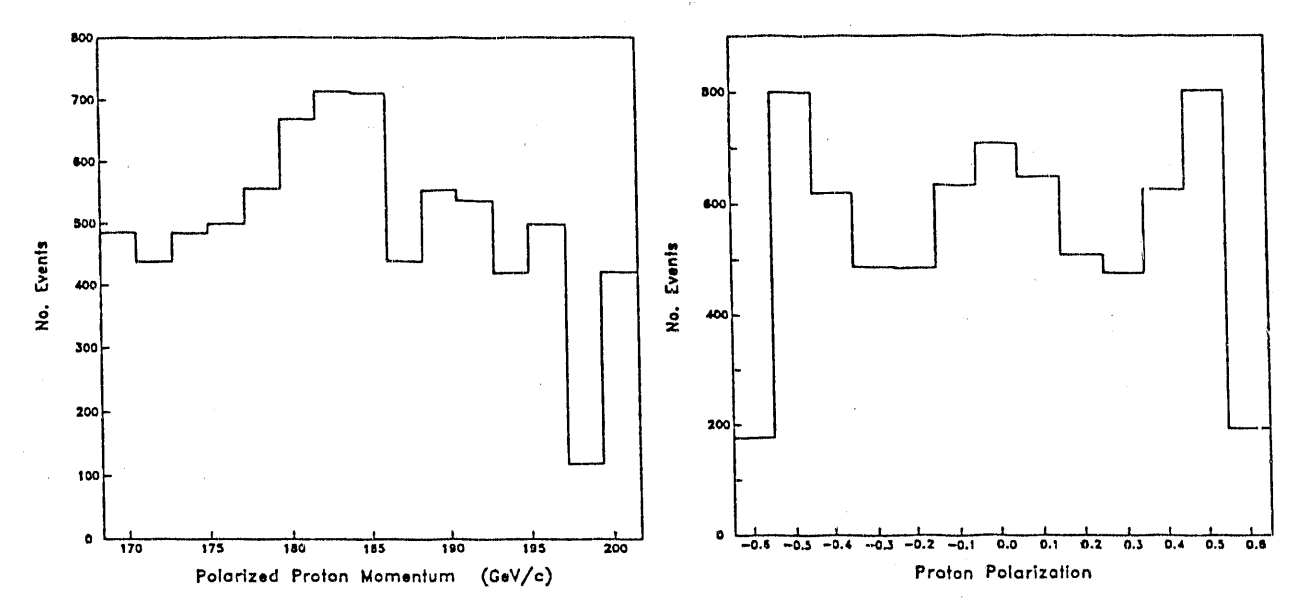


Figure 6: Typical plot of the polarized proton momentum measured by the beam-tagging system.

Figure 7: Typical plot of the proton polarization measured by the beam-tagging system.

within 250 ns by the electronics, with the signals being sent to the experimental triggers. The hodoscopes use an overlapping design of the scintillators for more segmentation and an improved position measurement.

A plot of the beam momentum, as measured by the beam-tagging system, is given in Fig. 6. The central-momentum value of $185 \, \text{GeV/c}$ (used at the time of this measurement) with the $\pm 9\%$ momentum bite and the finite-size effects of the scintillators are seen in this figure. The momentum resolution is estimated to be approximately 1.5% (rms). Figure 7 shows the proton polarization measured from -65 to +65% in intervals of 10% by the beam-tagging system. The polarization resolution is estimated to be 11%. Particles with polarization values measured between +35% and +65% are designated "positive," those with values between -35% and -65% are "negative," and those between -35% and +35% are labeled as "zero." Similar results are obtained for the polarized antiproton beam.

C. The Beam Polarimeters

The beam-tagging system assigns a polarization value to each beam particle using a position relative to a known trajectory. In order to verify that the beam is indeed polarized and that the polarization as measured by the tagging method is correct, measurements were performed by two different beam polarimeters developed for high-energy

particles. The first one uses the dissociation of polarized protons in the Coulomb field of a heavy nucleus, the Primakoff effect, and the second one uses the Coulomb-nuclear interference in the elastic scattering of polarized protons by a proton target. Only a brief description of the polarimeter and the measurements will be made here.

The Primakoff-effect polarimeter gives the beam polarization by measuring the asymmetry in coherent Coulomb dissociation,³ in which an incident proton is converted to a $p-\pi^0$ system in the Coulomb field of a high-Z, nuclear target. This reaction when produced at high energy, is related to the low-energy photoproduction of a π^0 from a proton. The beam polarization can then be determined from the low-energy data⁴ and the measured asymmetry.

The polarimeter consists of a Pb target, a segmented lead glass calorimeter, and a magnetic spectrometer. The lead glass calorimeter detects the two photons from the π^0 decay, and provides both energy and position information. The magnetic spectrometer, made up of wire chambers, scintillation counters, and an analyzing magnet, determine the momentum of the proton. A vertically-polarized proton beam was incident on the target and a left-right asymmetry was observed in the polarimeter.

The π^0 is reconstructed along with the proton trajectory to determine the mass of the p- π^0 system. Events having a mass between 1.36 and 1.52 GeV/ c^2 are selected because this mass range contains the largest analyzing power. Events with a momentum transfer squared less than 10^{-3} (GeV/c)² are also chosen because this region is where the Primakoff process is large. The raw left-right asymmetry was measured⁵ as $-(14 \pm 3)\%$ for surviving events with tagged polarization greater than 35%. The average beam polarization was then determined to be $(40 \pm 9 \pm 15)\%$, compared to 45% given by the beam-tagging system. The first error is statistical and the second is due to the uncertainty in subtracting out the background processes. Consistency checks of the data measured in regions outside that of the Primakoff process and that of large analyzing power, and also for zero tagged polarization all showed no asymmetry. The Primakoff process was observed using polarized antiprotons, but not enough data were collected to determine the beam polarization. This polarimeter has demonstrated the polarization of the beam and verified the beam-tagging polarization measurements.

The Coulomb-nuclear interference polarimeter gives the beam polarization by measuring the asymmetry in proton-proton elastic scattering using a polarized proton beam in the interference region of the momentum transfer squared, t, from 1 to $30 \times 10^{-3} \, (\text{GeV/c})^2$. The analyzing power for the process is due to the interference term between the nuclear non-flip amplitude and the electromagnetic spin-flip amplitude. This process is virtually independent of the energy.

This polarimeter consists of seven scintillator targets, two scintillator hodoscopes

upstream of the target, a transmission hodoscope, twelve wire chambers, and an analyzing magnet. The two upstream hodoscopes define the vertically-polarized particle trajectory upstream of the target, while the other detectors comprise a magnetic spectrometer that measures the scattered particle's momentum. The scintillator target uses pulse height to distinguish a recoil proton from a transmitted one. A correlation between the scintillator pulse height and the |t| value of the scattered particle is used to select elastically-scattered events.

The |t| value is calculated from the spatial difference in both the horizontal and vertical directions between a projected position and the actual position. If the difference is too small, the particle is designated as not interacting in the target and the event is rejected. By requiring both a recoil proton from the target and a $|t| > 0.001 \, (\text{GeV/c})^2$, a total of 36 000 events were found. Using the measured left-right asymmetry over the range, $0.001 < |t| < 0.03 \, (\text{GeV/c})^2$ and average analyzing power of 3.7%, the beam polarization was found to be $(41 \pm 26)\%$, compared to the beam-tagging value of 42%. Data checks yielded no asymmetry for particles whose polarization was tagged as zero and also for an up-down asymmetry measurement. The results from this polarimeter, although limited by low statistics, are consistent with the average beam polarization by the beam-tagging system and the method has been demonstrated to work at high energies. A data-taking period in the summer of 1990 has resulted in a 15-fold increase in the statistics and the expected error on the asymmetry will be better than 1%.

D. The Experimental Program

The first set of experiments using the polarized proton and antiproton beams will be briefly listed. These experiments include: a measurement of the difference in total cross section between parallel and antiparallel helicity states ($\Delta \sigma_L$) for both p-p and \overline{p} -p interactions; the large transverse momentum production of neutral pions; the large- x_F inclusive production of pions, Λ and Σ hyperons; and the double spin asymmetry measurement of neutral pions using a longitudinally-polarized beam and target. All of these measurements acquired data during a period from February to August 1990. Possible future experiments will measure the direct photon and the χ_2 particle production using both a polarized beam and target. These measurements would provide information on the gluon contribution to the spin of the proton.

F. References

*Work supported by the U.S. Department of Energy, Division of High Energy Physics, Contract W-31-109-ENG-38.

†For the FNAL E-581/704 Collaboration: Argonne, CEN-Saclay, Fermilab, IHEP-Serpukhov, INFN-Messina, INFN-Trieste, Iowa, Kita-Kyushu, Kyoto, Kyoto Education, Kyoto-Sangyo, LAPP-Annecy, Los Alamos, Northwestern, Rice, Udine.

- ¹D. P. Grosnick et al., Nucl. Instrum. Methods A290, 269 (1990).
- ²J. W. Cronin and O. E. Overseth, Phys. Rev. 129, 1795 (1963).
- ³H. Primakoff, Phys. Rev. **81**, 899 (1951); A. Halprin, C. M. Andersen, and H. Primakoff, Phys. Rev. **152**, 1295 (1966).
 - ⁴M. Fukushima et al., Nucl. Phys. **B136**, 189 (1978).
 - ⁵D. C. Carey et al., Phys. Rev. Lett. **64**, 357 (1990).
- ⁶B. Z. Kopeliovich and L. I. Lapidus, Yad. Fiz. **19**, 218 (1974) [Sov. J. Nucl. Phys. **19**, 114 (1974)]; N. H. Buttimore, E. Gotsman, and E. Leader, Phys. Rev. D **18**, 694 (1978); J. Schwinger, Phys. Rev. **73**, 407 (1948).
 - ⁷N. Akchurin *et al.*, Phys. Lett. **B229**, 299 (1989).

DISCLAIMER

This report was prepared as an account of work sponsored by an agency of the United States Government. Neither the United States Government nor any agency thereof, nor any of their employees, makes any warranty, express or implied, or assumes any legal liability or responsibility for the accuracy, completeness, or usefulness of any information, apparatur, product, or process disclosed, or represents that its use would not infringe privately owned rights. Reference herein to any specific commercial product, process, or service by trade name, trademark, manufacturer, or otherwise does not necessarily constitute or imply its endorsement, recommendation, or favoring by the United States Government or any agency thereof. The views and opinions of authors expressed herein do not necessarily state or reflect those of the United States Government or any agency thereof.

DATE FILMED 02/08/19/